

# A Study on Fuzzy Logic Based Intelligent Control of Robot System to Improve the Work Efficiency for Smart Factory

Hee-Jin Kim<sup>1\*</sup>, Dong-Ho Kim<sup>1</sup>, Sung-Hyun Han<sup>2</sup>

## 〈Abstract〉

In this paper, we propose a new approach to intelligent control based on fuzzy logic for work efficiency improvement of smart factory by the application of articulated robot. The intelligent control that is applied to the working process by the joint of robotic manipulator is the main focus to improve a work efficiency for implementation of smart factory in general manufacturing process. In this study, we propose a new method of a fuzzy model and then develop a nonlinear relationship between interaction forces and manipulator position using a fuzzy model. The reliability of the proposed control method is illustrated by simulation and experiments.

*Keywords : Intelligent Control, Work Efficiency Improvement, Implimentation of Smart Factory, Articulated Robot*

---

<sup>1\*</sup> Dept.of Mechanical Couvergence Engineering, Graduate School, Kyungnam University, Changwon, Korea  
Tel: \*\*\* - \*\*\*\* - \*\*\*\*    \*\*\* - \*\*\*\* - \*\*\*\*    E-mail: jizhen@nate.com, k2971845@naver.com

<sup>2</sup> School of Mechanical Engineering, Kyungnam University, Changwon, Korea

## 1. Introduction

In general, the intelligent control of robot system has been recognized as an essential robot capability, but the actual implementation has been delayed due to parameter uncertainty and system instability.

One of the reasons for the difficulties of the stable control is that the characteristic of the environment that a robot contacts is uncertain. Therefore it is necessary to estimate the environmental parameters to improve the performance of position velocity, and force control[1].

Usually, environmental condition becomes progressively complication as they are deflected and it is necessary to determine a accurate function. For that, first we propose a new method of a fuzzy model and then develop a nonlinear relationship between interaction forces and manipulator position using a fuzzy model. By controlling the manipulator position and specifying its relationship to the interaction forces, we can ensure that the manipulator is able to maneuver in a constrained environment while maintaining to maneuver in a constrained environment while maintaining appropriate contact force. In general, the system nominal stability for  $n$  degree-of-freedom manipulator is proved theoretically using Lyapunov's direct method[2].

manipulator is controlled with the guarantee of stability.

## 2. System Modeling

In this work, we derive kinetic equations using Lagrangian methods using the work and energy terms of the system. If the system's generalized coordinate system is referred to as, and the and are referred to as total kinetic and positional energy, respectively, the Lagrangian can be defined as follows.

$$L(\theta_i, \dot{\theta}_i) = T(\theta_i, \dot{\theta}_i) - U(\theta_i, \dot{\theta}_i) \quad (i = 1, 2, \dots, n) \quad (2.1)$$

Describe the equations of motion in the system as follows[3].

$$\frac{d}{dt} \left( \frac{\partial L}{\partial \dot{\theta}_i} \right) - \frac{\partial L}{\partial \theta_i} = Q_i \quad (i = 1, 2, \dots, n) \quad (2.2)$$

Here, it represents a generalized force applied in the direction of generalized coordinates. Generalized forces can be obtained by considering the virtual task of non-preserving forces applied to the system.

### 2.1 Inertial matrix of the manifold

In order to induce the equation of motion, kinetic and positional energy of all joints must be obtained.

It represents the velocity vector and angular velocity vector in the base coordinate system from Fig. 2-1. The kinetic energy of the link and the system as a whole are as follows[4].

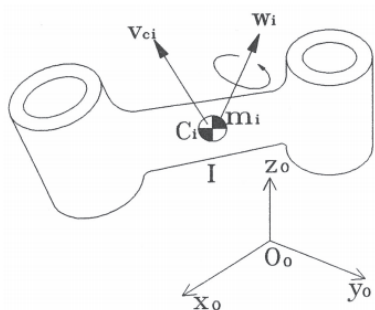


Fig. 2 The velocity and acceleration of mass center of link I

$$T_i = \frac{1}{2} m_i v_{ci}^T + \frac{1}{2} w_i^T I_i w_i \tag{2.3}$$

$$T = \sum_{i=1}^n T_i$$

where represents the mass of the link, and the represents the moment of inertia (33) to the center of mass. In expression (2.3), the first term represents parallel kinetic energy, and the second term represents rotational kinetic energy[4].

In expression (2.3), kinetic energy is represented by the velocity and angular velocity of a dependent link, which is a generalized coordinate, articulated displacement, velocity, angular velocity and Jacobian matrix in equation (2.3).

$$v_{ci} = J_{L1}^{(i)} \dot{\theta}_1 + \dots + L_{Li}^{(i)} \dot{\theta}_i = J_L^{(i)} \dot{\theta}$$

$$w_{ci} = J_{A1}^{(i)} \dot{\theta}_1 + \dots + L_{Ai}^{(i)} \dot{\theta}_i = J_A^{(i)} \dot{\theta} \tag{2.4}$$

This is the first column vector with the Jacobian matrix of parallel and rotational speeds of Link I, respectively. This is represented by a matrix as follows[5].

$$J_L^{(i)} = [ L_{L1}^{(i)} \dots J_{Li}^{(i)} 0 \dots 0 ]$$

$$J_A^{(i)} = [ L_{A1}^{(i)} \dots J_{Ai}^{(i)} 0 \dots 0 ] \tag{2.5}$$

Since the movement of the link is influenced by joints from one to one, the abnormal joint column vector becomes zero. These include :

$$J_{Lj}^{(i)} = \begin{cases} b_{j-1} & \\ b_{j-1} \times r_{j-1,ci} & \end{cases} \quad J_{Aj}^{(i)} = \begin{cases} 0 & \\ b_{j-1} & \end{cases} \tag{2.6}$$

where is the position vector of the link mass zoom core to the coordinate system, and the is the unit vector of the joint axis.

Equation (2.4) is substituted for formula (2.3).

$$T = \frac{1}{2} \sum_{i=1}^n (m_i \dot{\theta}^T J_L^{(i)T} J_L^{(i)} \dot{\theta} + \dot{\theta}^T J_A^{(i)T} I_i J_A^{(i)} \dot{\theta})$$

$$= \frac{1}{2} \dot{\theta}^T H \dot{\theta} \tag{2.7}$$

Here, the inertial matrix of the manifold is as follows.

$$H = \sum_{i=1}^n (m_i J_L^{(i)T} + J_A^{(i)T} I_i J_A^{(i)}) \tag{2.8}$$

The inertial matrix of the manifold differs from the inertial moment of the link, but has similar properties. In other words, the inertial matrix of the manifold is symmetrical halve, such as the moment of inertia, and has a quadratic form. In expression (2.8) the inertial matrix of the manifold varies with the shape of the manifold because it contains

the Jacobian matrix.

The following is a rephrase of expression (2.7) when referring to the element of .

$$T = \frac{1}{2} \sum_{i=1}^n \sum_{j=1}^n H_{ij} \dot{\theta}_i \dot{\theta}_j \quad (2.9)$$

### 2.2 Induction of equations of motion

In order to induce kinetic equations in Lagrangian law, must obtain kinetic energy, positional energy, and generalized forces. The gravitational acceleration vector for the reference coordinate system is as follows[5].

$$U = \sum_{i=1}^n m_i g^T r_{o,ci} \quad (2.10)$$

Here, since the link-centric vector varies with the robot's geometry, position energy is a function of joint displacement.

Generalized forces are all forces applied to the link except gravity and inertia. This can be thought of as an external force when torque and terminal effectors applied to each joint come into contact with objects in the environment. Generalized forces are obtained by calculating the hypothetical task of these forces. The virtual jobs are as follows:[5]

$$\delta W = \tau^T \delta \theta + F_{ext}^T \delta p = (\tau + J^T F_{ext})^T \delta \theta \quad (2.11)$$

The relationship between virtual work and generalized power is as follows:

$$\delta W = \theta^T \delta \theta \quad (2.12)$$

The generalized forces in expressions 2.11 and 2.12 are as follows.

$$Q = \tau + J^T F_{ext} \quad (2.13)$$

The kinetic energy, positional energy, and generalized forces obtained from the above can be used to derive the kinetic equation. Calculation of expression (2.9) in the form of the first paragraph of expression (2.2) is as follows:[6]

$$\begin{aligned} \frac{d}{dt} \left( \frac{\partial T}{\partial \dot{\theta}_i} \right) &= \frac{d}{dt} \left( \sum_{j=1}^n H_{ij} \dot{\theta}_j \right) \\ &= \sum_{j=1}^n H_{ij} \ddot{\theta}_j + \sum_{j=1}^n \frac{dH_{ij}}{dt} \dot{\theta}_j \end{aligned} \quad (2.14)$$

In expression (2.14), since it is a function, the differential term is as follows.

$$\frac{dH_{ij}}{dt} = \sum_{k=1}^n \frac{\partial H_{ij}}{\partial \theta_k} \frac{d\theta_k}{dt} = \sum_{k=1}^n \frac{\partial H_{ij}}{\partial \theta_k} \dot{\theta}_k \quad (2.15)$$

The second paragraph in formula (2.2) contains partial differential terms of kinetic energy, which are as follows:

$$\begin{aligned} \frac{\partial T}{\partial \dot{\theta}_i} &= \frac{\partial}{\partial \dot{\theta}_i} \left( \frac{1}{2} \sum_{j=1}^n \sum_{k=1}^n H_{jk} \dot{\theta}_j \dot{\theta}_k \right) \\ &= \frac{1}{2} \sum_{j=1}^n \sum_{k=1}^n \frac{\partial H_{jk}}{\partial \dot{\theta}_i} \dot{\theta}_j \dot{\theta}_k \end{aligned} \quad (2.16)$$

The term of gravity is obtained by partial differentiation of positional energy as follows.

$$\begin{aligned} G_i &= \frac{\partial U}{\partial \theta_i} = \sum_{j=1}^n m_j g^T \frac{\partial r_{o,cj}}{\partial \theta_i} \\ &= \sum_{j=1}^n m_j g^T J_{Li}^{(j)} \end{aligned} \quad (2.17)$$

Equations (2.14),(2.15),(2.16) and 2.17) are substituted for Equations (2.2).

$$\sum_{j=1}^n H_{ij} \ddot{\theta}_j + \sum_{j=1}^n \sum_{k=1}^n V_{ijk} \dot{\theta}_j \dot{\theta}_k + G_i = Q_i \quad (i = 1, 2, \dots, n) \quad (2.18)$$

It's  $V_{ijk} = \frac{\partial H_{ij}}{\partial \theta_k} - \frac{1}{2} \frac{\partial H_{jk}}{\partial \theta_i}$  here. The first term of expression (2.18) represents inertia terms, the second term represents Coriolis and centrifugal forces, and the third term represents gravity terms, respectively.

### 3. Control Scheme

The fuzzy logic controller must design control rules through trial and error attempts and modification processes until satisfactory performance is achieved through repeated experiments. Although modification methods of systematic control rules are proposed, these tasks are tedious. Therefore, a controller is required to adjust the control rules on its own so that the system can exert the desired output. To this end, we propose a novel self-organizing fuzzy controller (SOFC). A self-configuring fuzzy controller performs two tasks simultaneously.

- [i] Observe the environment while outputting appropriate control inputs.
- [ii] Improve the following results by utilizing the results from control inputs.

In other words, it is an integration of identification and control of the system. With

a self-configuration fuzzy controller, a controller can be designed with minimal information about the environment. Fig. 3-19 represents the overall structure for the entire robotic manifold consisting of the proposed self-configuration fuzzy controller. And the structure of the magnetic composition fuzzy controller is Fig. It is shown in 3-20. As in Fig. 3-20, performance adds parts, adjustment factor modification parts, and rule modification parts to give existing simple fuzzy controllers and automatic joint capabilities[7].

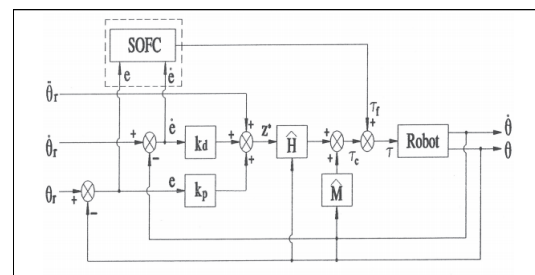


Fig. 3.1 The block diagram of proposed fuzzy control structure for robot manipulator

The fuzzy logic controller must design control rules through trial and error attempts and modification processes until satisfactory performance is achieved through repeated experiments. Although modification methods of systematic control rules are proposed, these tasks are tedious. Therefore, a controller is required to adjust the control rules on its own so that the system can exert the desired output. To this end, we propose a novel self-organizing fuzzy controller (SOFC). A self-configuring fuzzy controller performs two tasks simultaneously.

In order to compensate for errors arising from structural uncertainty and unstructured uncertainty, the following can be defined from the equations of motion of the experimental robot[8].

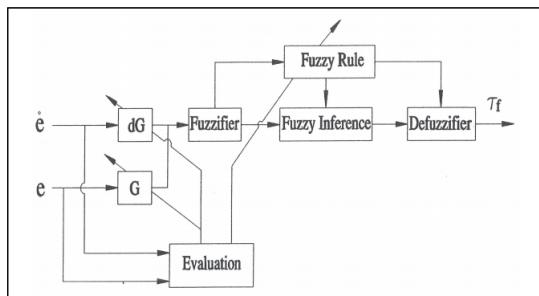


Fig. 3.2 The block diagram of structure for self organizing fuzzy controller

By definition, when applied as an output signal from a purge controller, the right-hand side is increasingly hydrophobic and approaches the ideal system.

If the control input is updated to achieve the same result as and then the right-hand variable term is zero as an ideal state. By this principle, the final output is added or subtracted by the output from the self-configuration fuzzy controller and gradually the right-hand side converges to zero, thus approaching the ideal system. A. Calibration amount inference of self-configuration fuzzy controllers. At the sample moment of the output of the plant by the input is generated. If the output requirements were generated by the model. This value is the error between the reference input and the plant output at each sample time. The inference process of

the correction amount uses a method that outputs already set values with errors, without exploiting existing inference methods. The fuzzy variables used at this time are as follows[9].

IF is PN then PB

IF is PS then PS

IF is ZERO then ZERO

IF is NS then NS

IF is NB then NB

is the value of 30% of the output generated by the fuzzy controller. B Modification of the basic rules of the self-configuration fuzzy controller.

When improving the performance of fuzzy controllers, the modification of rules is largely divided into three methods[10].

- Modify control rules
- Modification of scaling factors
- Correct control rules and gain terms at the same time

Here, the second method can improve the control performance of the system, but the premise is that the appropriate fuzzy control rules are preset. The third such change method can also improve the performance of the system, but the question of how to properly change the two components of control rules and coordinators at the same time remains a research challenge. A typical self-configuration fuzzy controller relies on the modification of the first method, control rules. This research paper not only changes the rules but also modifies the co-ordinator at the same time[9].

## 4. Performance Test and Results

### 4.1 Simulation and results

To verify the reliability of the control performance of the proposed self-configuration Fuzzy controller, simulations are performed on the eight-freedom plane rotation joints of the Scar-type dual arm robot. We perform with only 1 and 2 joints considered in the dynamic equation of the Scar-type robot defined in the battlefield. Scar-type robots are given the greatest weight to the joints of 1 and 2, and the reliability of the control algorithm can be sufficiently verified without including the joints of 3 and 4.

Looking at the terms of each element, we find that the robot's kinetic equation is feature dependent, as each link contains a perminator variable. Coriolis and centrifugal forces can be induced using the preceding inertial matrix  $H$ , first of all, the general expression of the coriolis and centrifugal force terms is as follows.

Here, for each term ( $i, j, k = 1, 2, 3, 4$ ) by applying it to a Scarra-type robot, the terms that do not have zero values are as follows.

Furthermore, is the weight of the load on the terminal effect device, which can be seen in real-world systems where constant work is always done, but unknown load is given in case of performing work. In this simulation, we increase these unknown loads from 1 kg to 4 kg to confirm the reliability of the

performance of the proposed controller.

By definition, when applied as an output signal from a purge controller, the right-hand side is increasingly hydrophobic and approaches the ideal system. If the control input is updated to achieve the same result as and then the right-hand variable term is zero as an ideal state. By this principle, the final output is added or subtracted by the output from the self-configuration fuzzy controller and gradually the right-hand side converges to zero, thus approaching the ideal system.

This value is the error between the reference input and the plant output at each sample time. The inference process of the correction amount uses a method that outputs already set values with errors, without exploiting existing inference methods[9].

The fuzzy variables used at this time are as follows.

IF is PN then PB

IF is PS then PS

IF is ZERO then ZERO

IF is NS then NS

IF is NB then NB

is the value of 30% of the output generated by the purge controller.

B Modification of the basic rules of the self-configuration fuzzy controller.

When improving the performance of fuzzy controllers, the modification of rules is largely divided into three methods.

- 1) Modify control rules
- 2) Modification of scaling factors
- 3) Correct control rules and gain terms at the same time.

Here, the second method can improve the control performance of the system, but the premise is that the appropriate fuzzy control rules are preset. The third such change method can also improve the performance of the system, but the question of how to properly change the two components of control rules and coordinators at the same time remains a research challenge. A typical self-configuration fuzzy controller relies on the modification of the first method, control rules. This research paper not only changes the rules but also modifies the co-ordinator at the same time[9][10][14].

The modification of the co-ordinator takes the output of the number of runs in accordance with the initial rule and normalizes the fudge value between -6 and 6. The reason for correcting the adjustment factor is that it is difficult to find the exact amount of error and error change in vibrating targets, such as flexible manifolds. If the value is not correctly found, it may be normalized only near the ZO, or it may otherwise exceed -6 and 6. In this case, it is difficult to apply the rules accurately. When the results of the execution with the initial rules come out, they find the correct adjustment factor and apply it with a number of new rules that have been fuzzy[9][10][15].

In this study, The sampling time is one msec and performed for 2 seconds to achieve better performance by simultaneously varying the coordinator and posterior rules. The funny variable in the simulation was used an equidistant trigonometric function, and the initial rules

were shown in Table 4.1. The previously inferred is combined with the by an initial rule to infer a new output, and the gain is multiplied by each corresponding sampling time. The table shows the specifications of each ink. To confirm the performance of the proposed controller, we analyze the results by applying them to the experimental horizontal type Robot manipulator by increasing the load on the reference input of the gentle slope. The sampling time was 1 msec and performed for 2 seconds to achieve better performance by simultaneously varying the coordinator and posterior rules. The main variable in the simulation is used an equidistant trigonometric function, and the initial rules were shown in Table 4.1. The Fig.4.1 shows the membership values for the linguistic variable. To confirm the performance of the proposed controller, analyze the results of simulation[11][12][13].

**Table. 4.1 Membership for linguistic variable**

	NB	NM	NS	ZO	PS	PM	PB
-6	1	0.3	0	0	0	0	0
-5	0.7	0.7	0	0	0	0	0
-4	0.3	1	0.3	0	0	0	0
-3	0	0.7	0.7	0	0	0	0
-2	0	0.3	1	0.3	0	0	0
-1	0	0	0.7	0.7	0	0	0
0	0	0	0.3	1	0.3	0	0
1	0	0	0	0.7	0.7	0	0
2	0	0	0	0.3	1	0.3	0
3	0	0	0	0	0.7	0.7	0
4	0	0	0	0	0.3	1	0.3
5	0	0	0	0	0	0.7	0.7
6	0	0	0	0	0	0.3	1



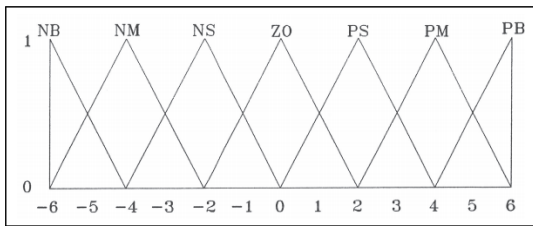


Fig. 4.1 Linguistic variable

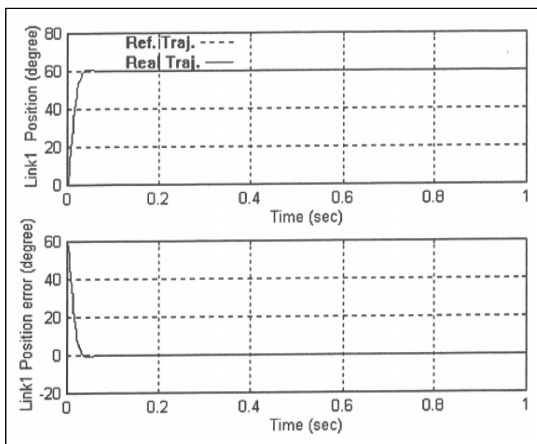


Fig. 4.2 Simulation results of position trajectory tracking for the link 1 with noload in case of step input

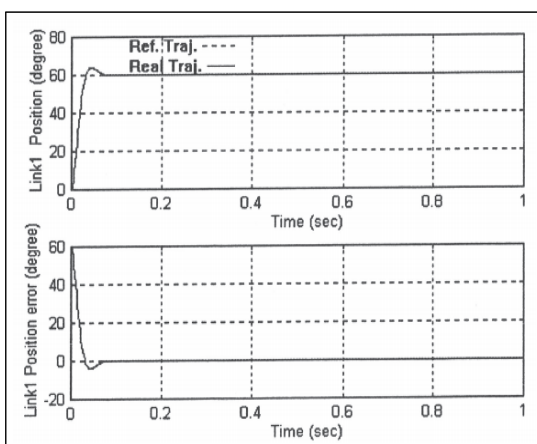


Fig. 4.3 Simulation results of position trajectory tracking for link 1 with 2kg payload in case of step funtion input

### 4.1.1 Simulation Results

From Fig.4.2 to Fig.4.12, it can be verified the results of the performance test of the proposed controller at no load, 2kg, and 4kg load states of joints. and can be found to have relatively good control performance. Fig. 4.2 represents the experimental results of position trajectory tracking for the link 1 with noload in case of step input. Fig. 4.3 represents the experimental results of position trajectory tracking for the link 1 with 2kg load in case of step input, From this simulation

Fig. 4.4 represents the experimental results of position trajectory tracking for the link 1 with 4kg load in case of step input. Fig. 4.5 represents the experimental results of position trajectory tracking for the link 2 with no load in case of step input. Fig. 4.6 represents the experimental results of position trajectory tracking for the link 2 with 2kg load in case of step input. Fig. 4.7 represents the experimental results of position trajectory tracking for the link 2 with 4kg load in case of step input. Fig. 4.8 shows the simulation results of position and velocity trajectory tracking for link 1 with noload in case of ramp input. Fig. 4.9 shows the simulation results of position and velocity trajectory tracking for link 1 with 2kg payload in case of ramp input Fig. 4.10 shows the simulation results of position and velocity trajectory tracking for link 1 with 3kg in case of sinusoidal input Fig. 4.11 represents the simulation results of position and velocity trajectory tracking for link 2 with noload in case of sinusoidal input

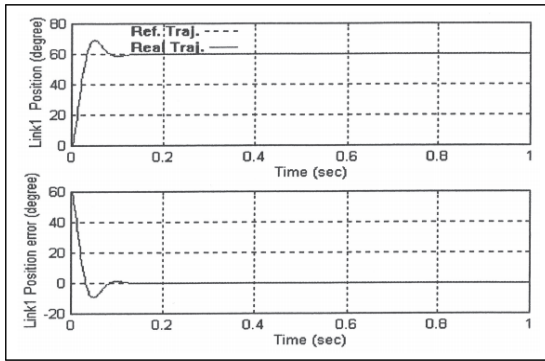


Fig. 4.4 Simulation results of position trajectory tracking for link 1 with 4kg payload in case of step input

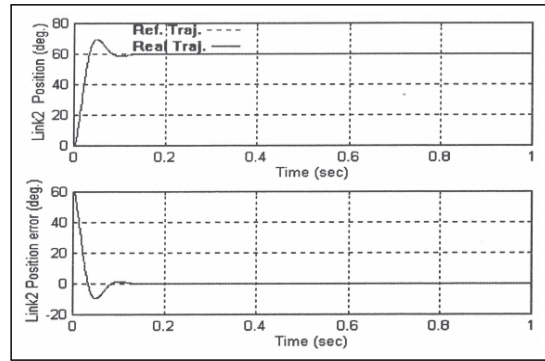


Fig. 4.7 Simulation results of position trajectory tracking for link 2 with 4kg payload in case of step input

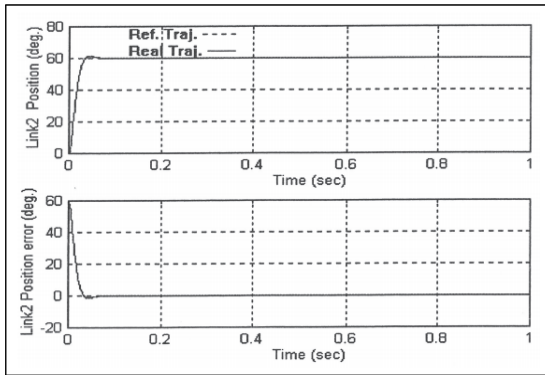


Fig. 4.5 Simulation results of position trajectory tracking for link 2 with no-load in case of step input

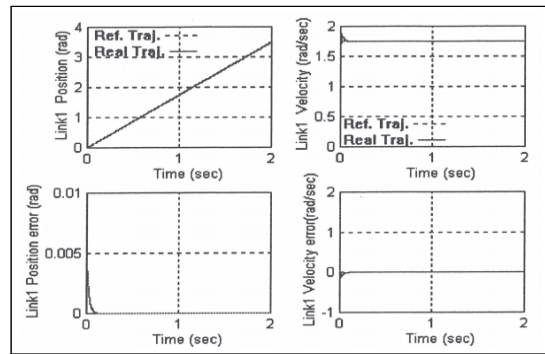


Fig. 4.8 Simulation results of position and velocity trajectory tracking for link 1 with no-load in case of ramp input

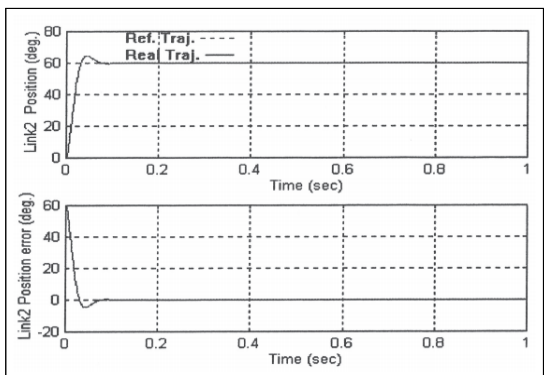


Fig. 4.6 Simulation results of position trajectory tracking for link 2 with 2kg payload in case of step function input

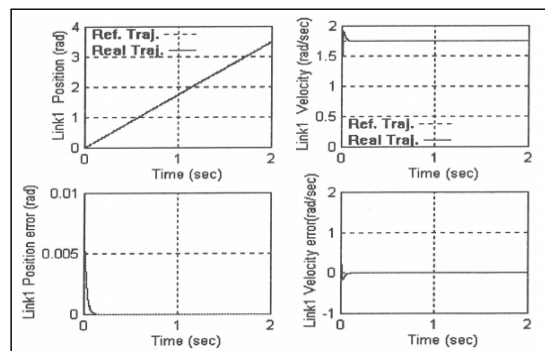


Fig. 4.9 Simulation results of position and velocity trajectory tracking for link 1 with 2kg payload in case of ramp input

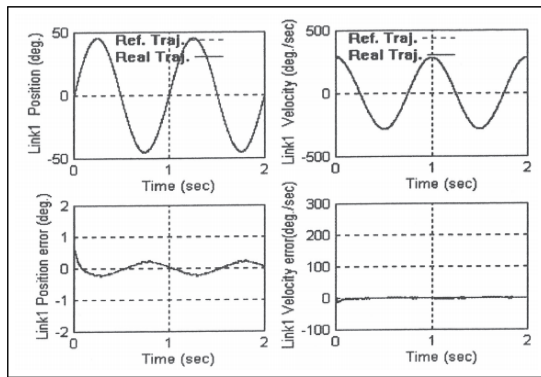


Fig. 4.10 Simulation results of position and velocity trajectory tracking for link 1 with 3kg in case of sinusoidal input

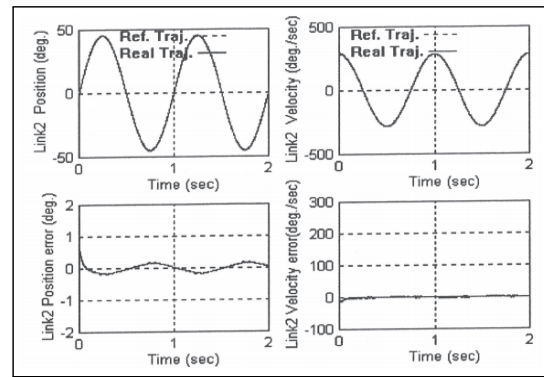


Fig. 4.12 Simulation results of position and velocity trajectory tracking for link 2 with 3kg in case of sinusoidal input

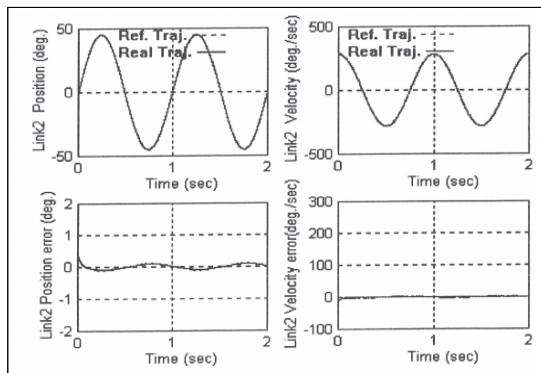


Fig. 4.11 Simulation results of position and velocity trajectory tracking for link 2 with noload in case of sinusoidal input

Fig. 4.12 shows the simulation results of position and velocity trajectory tracking for link 2 with 3kg in case of sinusoidal input

As shown in the figure, we could confirm that the simulation results showed very good performance in trajectory tracking under the various conditions.

Therefore, the simulation results showed the validity of the control algorithm of the proposed fuzzy controller.

Fig. 4.4 represents the experimental results of position trajectory tracking for the link 1 with 4kg load in case of step input. Fig. 4.5 represents the experimental results of position trajectory tracking for the link 2 with no load in case of step input. Fig. 4.6 represents the experimental results of position trajectory tracking for the link 2 with 2kg load in case of step input. Fig. 4.7 represents the experimental results of position trajectory tracking for the link 2 with 4kg load in case of step input. Fig. 4.8 shows the simulation results of position and velocity trajectory tracking for link 1 with noload in case of ramp input. Fig. 4.9 shows the simulation results of position and velocity trajectory tracking for link 1 with 2kg payload in case of ramp input Fig. 4.10 shows the simulation results of position and velocity trajectory tracking for link 1 with 3kg in case of sinusoidal input Fig. 4.11 represents the simulation results of position and velocity trajectory tracking for link 2 with noload in case of sinusoidal

input. Fig. 4.12 shows the simulation results of position and velocity trajectory tracking for link 2 with 3kg in case of sinusoidal input. As shown in the figure, we could confirm that the simulation results showed very good performance in trajectory tracking under the various conditions. Therefore, the simulation results showed the validity of the control algorithm of t proposed control method.

### 4.2 The Experiment and Results

Fig. 4.13 shows the experimental set-up of horizontal type robot system based on monitoring simulator. Fig. 4.14 shows the experiment results of joint 1 by roposed control method based on monitoring simulator with 3kg. load. Fig. 4.15 e shows the xperiments results of joint 2 by proposed control method based on monitoring simulator with 3kg load. Fig. 4.16 shjows the experiment results of joint 3 by proposed control method based on monitoring simulator with 3kg load.



Fig. 4.13 Experimental set-up of horizontal type robot system based on monitoring simulator

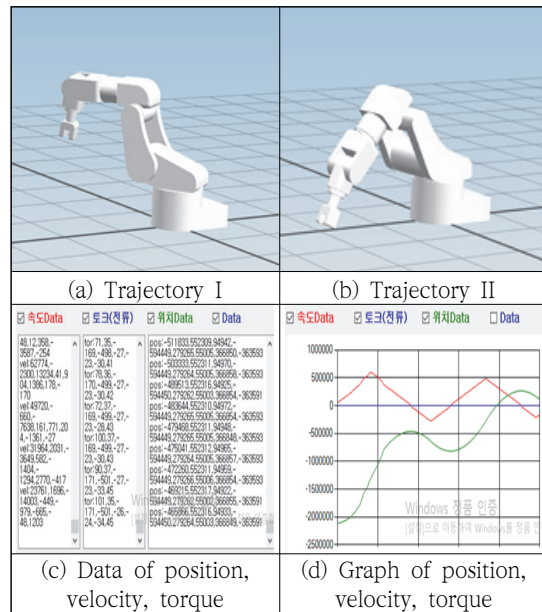


Fig. 4.14 Experiment results of joint 1 by the roposed control method based on monitoring simulator with 3kg load

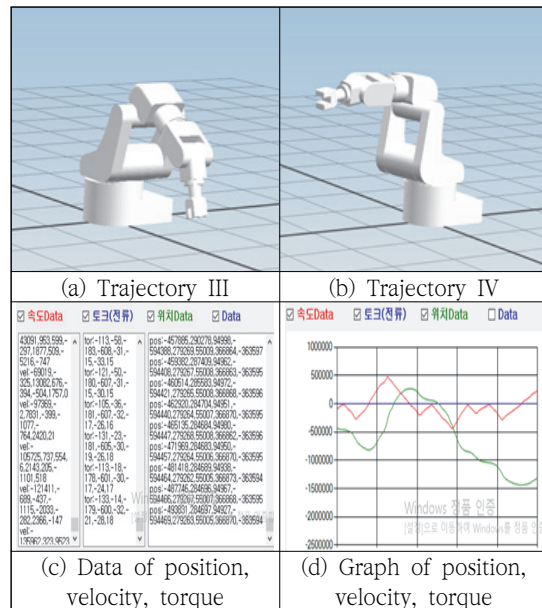


Fig. 4.15 Experiments results of joint 2 by proposed control method based on monitoring simulator with 3kg load



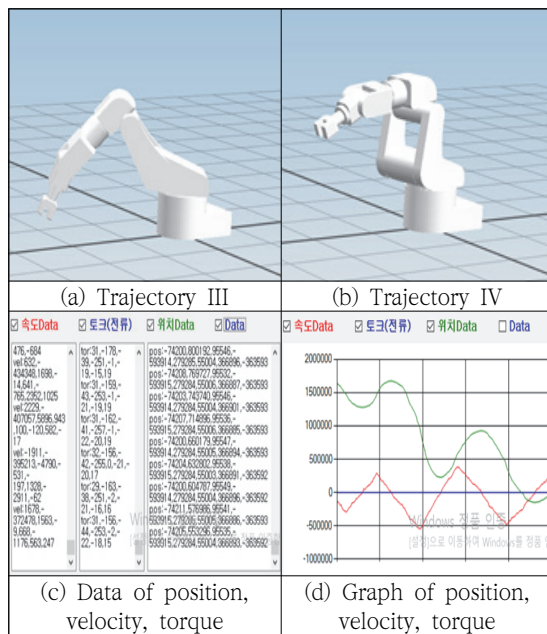


Fig. 4.16 Experiment results of joint 3 by proposed control method based on monitoring simulator with 3 kg load

## 5. Conclusions

This study proposed a new approach to intelligent control technology based on fuzzy logic model for work efficiency improvement of smart factory by articulated robot system.

The proposed control method was constructed as a scheme of self-organizing fuzzy controller.

The self-organizing fuzzy logic controller was designed based on basic control rules through trial and error attempts and modification processes until satisfactory performance was achieved through repeated experiments.

The performance of proposed intelligent control method was illustrated by simulation

and experiments based monitoring simulator under the various conditions variations,

From performance test results, the proposed method has been varified to have less steady-state error than the conventional one.

## Acknowledgement

This study was supported by Industrial Technology Innovation Project (Project Number: 20005020).

## References

- [1] An, C. H., and Hollerbach, J. M. "Dynamic stability issues in force control of manipulators," IEEE Int. Conf. Robotics Autom, Raleigh, NC, pp. 890-896, Mar. 31-Apr. 3, 1987.
- [2] J. Kenneth Salisbury, Jr., "Active stiffness Control of A Manipulator in Cartesian Coordinates," in 19th IEEE Conf. Decision and Control, pp.95-100, Dec., 1980.
- [3] F. L. Lewis, C. T. Abdallah, and D. M. Dawson, Control of Robot Manipulators, New York, MacMillan Publishing Company, 1993.
- [4] M. H. Raibert, J. J. Craig, "Hybrid Position/Force Control of Manipulator," Trans. ASME, vol. 102, pp. 126133, jun., 1981.
- [5] R. Volpe, "A Theoretical and Experimental Investigation of Impact Control for Manipulators," Int. J. Robotics Res, pp. 351-365, 1993.
- [6] Robert J. Anderson and Mark W. Spong, "Hybrid Impedance Control of Robotic Manipulators," IEEE Trans. Robotics Autom, vol. 4, no. 5, pp.549 - 556, Oct. 1988.
- [7] T. Takagi and M. Sugeno, "Fuzzy Identification

- of Systems and Its Applications to Modeling and Control," IEEE Trans. Systems, Man and Cybernetics, vol. SMC-15, no. 1, pp. 116-132, 1985.
- [8] M. Sugeno and G. T. Kang, "Structure Identification of Fuzzy Model," Fuzzy Sets and Systems, vol. 28, pp. 15-33, 1988.
- [9] M. Sugeno and T. Yasukawa, "A Fuzzy-Logic-Based Approach to Qualitative Modeling," IEEE Trans. Fuzzy
- [10] H.J. Kim, G.H. Dong, D.H. Kim, G.W. Jang and S.H. Han, "A Study on Track Record and Trajectory Control of Articulated Robot Based on Monitoring Simulator for Smart Factory", KSIC.2020.23.2 pp. 149-161
- [11] H.J. Kim, G.W. Jang, D.H. Kim and S.H. Han, "A Study on Track Record and Trajectory Control of Robot Manipulator with Eight Joints Based on Monitoring Simulator for Smart Factory", KSIC.2020.23.4 pp. 549-558
- [12] H.J. Kim, D.H. Kim, K.J. Jung and S.H. Han, "A Study on Performance Analysis of Articulated Robot System for Smart Factory Based on Monitoring Simulator", KSIC.2020.23.6 pp. 889-896
- [13] S.H. Kim, D. B. Kim, H.J. kim, O.D. Im and S.H. Han, "A Study on Real Time Control of Moving Stuff Action Through Iterative Learning for Mobile-Manipulator System", KSIC.2019.22.4 pp. 415-425
- [14] W.S. Lee, M.S. Kim, H.Y. Bae, Y.K. Jung, Y.H. Jung, G.S. Shin, I.M. Park and S.H. Han, "A Study on Stable Motion Control of Humanoid Robot with 24 Joints Based on Voice Command", KSIC.2018.21.1 pp. 17-27
- [15] H.S. Sim, H.Y. Bae, D.B. Kim and S.H. Han, "A Study on Flexible Control and Design of Robot Hand Fingers with Eight Axes for Smart Factory", KSIC.2018.21.4 pp. 183-189.

---

(Manuscript received July 19, 2021;

revised October 02, 2021; accepted October 06, 2021)